Ceramics International 42 (2016) 12202–12209

Contents lists available at ScienceDirect

Ceramics International

journal homepage: www.elsevier.com/locate/ceramint

Enhanced superconducting properties of $YBa_2Cu_3O_{7-\delta}$ thin film with magnetic nanolayer additions

Jijie Huang [a], Meng Fan [b], Han Wang [a], Li Chen [a], Chen-Fong Tsai [a], Leigang Li [a], Haiyan Wang [a,b,*]

[a] Department of Material Science and Engineering, Texas A&M University, College Station, TX 77843-3003, United States
[b] Department of Electrical and Computer Engineering, Texas A&M University, College Station, TX 77843-3128, United States

ARTICLE INFO

Article history:
Received 23 February 2016
Received in revised form
26 April 2016
Accepted 26 April 2016
Available online 27 April 2016

Keywords:
Flux pinning
Vertically aligned nanocomposite
Magnetic pinning

ABSTRACT

Vertically aligned nanocomposite (VAN) $(La_{0.7}Sr_{0.3}MnO_3)_{0.5}(CeO_2)_{0.5}$ and pure $La_{0.7}Sr_{0.3}MnO_3$ layers were incorporated into $YBa_2Cu_3O_{7-\delta}$ (YBCO) thin films as bilayer stacks for magnetic flux pinning enhancement. The films show high epitaxial quality, suggested by XRD and TEM study. The critical temperature $\mathbf{T_c}$ of the bilayers is about 90 K, which is close to that of pure YBCO films, while both the self-field $\mathbf{J_c^{sf}}$ and in-field critical current density $\mathbf{J_c^{in\text{-}field}}$ are largely enhanced. Among all samples, the film with VAN cap layer shows the highest $\mathbf{J_c}$ values in all field ranges. This study demonstrates an effective way towards the tunable pinning effect for YBCO coated conductors by both defect and magnetic pinning.

1. Introduction

Tremendous research efforts have been focused on the development of high temperature superconducting (HTS) coated conductors based on$YBa_2Cu_3O_{7-\delta}$ (YBCO) since it was discovered in 1987 [1–5]. Significant progress has been made first to address the needs on the epitaxial growth of the YBCO coated conductors on flexible metal substrates, and later to address critical issues that limit the performance of YBCO-based coated conductors. To enable the epitaxial growth of YBCO thin films on metal substrate, certain templates are required. The two primary approaches are (1) to involve a textured metal substrate to start with, i.e., rolling-assisted biaxially textured substrates (RABiTS) [5] and (2) to build an epitaxial template on amorphous buffered metal substrates called ion-beam-assisted deposition (IBAD) substrates [6–8]. Moreover, several film growth techniques have been successfully tailored for the deposition of YBCO thin films with high epitaxial quality on these metal substrates, such as metal-organic chemical vapor deposition (MOCVD) [9,10], pulsed laser deposition (PLD) [11–13], metal-organic deposition (MOD) [14,15] as well as magnetron sputtering [16,17]. With over a decade of development, superconducting properties of YBCO coated conductors have been significantly improved and practical applications have been demonstrated in multiple areas such as HTS coated conductors, superconductor magnets, generators and fault current limiters. [4,6,18,19] However, for most of the above technological applications, high critical current densities ($\mathbf{J_c}$) under applied magnetic field, so called in-field performance, is required.

Various flux pinning approaches have been introduced in YBCO HTS coated conductors to better pin flux lines and thus achieve superior $\mathbf{J_c}$ performance, in both self-field and in-field. Overall there are two categories, i.e., non-magnetic defect pinning and magnetic pinning. For non-magnetic defect pinning, most of the work has focused on the defect landscape design with various dimensional nanoinclusions, including nanoparticles [20,21], nanocolumns [22,23], as well as nanolayers [24]. Furthermore, some unique architectures were also designed, for example, Baca et al. combined Y_2O_3 nanoparticles and $BaZrO_3$ nanorods for overall pinning enhancement [25]. Magnetic pinning is another effective approach, because of the interaction between the magnetic inclusions and the fluxons [26–29]. Bulaevskiia et al. demonstrated that the high value of magnetic pinning potential $\mathbf{U_{mp}}$ ($\mathbf{U_{mp}\sim\Phi_0 M(x)d_s}$, where $\mathbf{M(x)}$ is the magnetization of the magnetic inclusion and $\mathbf{d_s}$ the thickness of the YBCO film) can overcome the thermal activated flux flow at high temperatures [30]. Various effective magnetic pinning centers have been demonstrated, including $CoFe_2O_4$ nanoparticle [31], CoPt layer [32], as well as $Pr_{0.67}Sr_{0.33}MnO_3$ (PSMO) layer [33].

In this study, a unique design of vertically aligned nanocomposite (VAN) layer embedding magnetic nanopillars was introduced into YBCO thin films as either cap layer or buffer layer for flux pinning enhancement. For demonstration, a VAN composite of CeO_2 and $La_{0.7}Sr_{0.3}MnO_3$ (LSMO) is selected. The selection of

* Corresponding author at: Department of Material Science and Engineering, Texas A&M University, College Station, TX 77843-3003, United States.
E-mail address: wangh@ece.tamu.edu (H. Wang).

http://dx.doi.org/10.1016/j.ceramint.2016.04.161
0272-8842/

LSMO: CeO_2 VAN as magnetic dopants is based on the excellent magnetic property of the LSMO phase [34–35] and that the in-plane lattice parameter of both LSMO (3.87 Å) and CeO_2 (5.411 Å with 45° rotation) is close to orthorhombic YBCO (a=3.82 Å, b=3.89 Å). Thus, both defect pinning and magnetic pinning effects are expected in this VAN nanolayer doped system. A pure LSMO layer buffered YBCO sample was also introduced for comparison.

2. Experimental

$(LSMO)_{0.5}(CeO_2)_{0.5}$ (L5C5)/YBCO and LSMO/YBCO bilayers were deposited by a PLD system with a KrF excimer laser (Lambda Physik 201, λ=248 nm, 300 mJ) on single crystal STO (001) substrates. The thickness of VAN nanolayer and YBCO matrix were controlled at about 20 nm (2 Hz, 2 min) and 350 nm (10 Hz, 6 min), respectively. The architecture of the bilayers thin films were prepared by alternative laser ablation of the nanocomposite and YBCO targets. The films were deposited with 300 mTorr oxygen in-flow at 780 °C, and followed by a post-annealing process under 300 Torr oxygen at 550 °C for 30 min

The microstructure of the films was characterized by X-ray diffraction (XRD) (PANalytical X'Pert X-ray diffractometer) and transmission electron microscopy (TEM) (FEI Tecnai G2 F20). The magnetization, critical transition temperature ($\mathbf{T_c}$), and critical current density (both $\mathbf{J_c^{sf}}$ and $\mathbf{J_c^{in\text{-}field}}$) were measured by a physical property measurement system (PPMS). $\mathbf{J_c^{in\text{-}field}}$ ($\mathbf{H//c}$) were measured under an applied field of 0–5 T at 77 K, 65 K, 40 K, and 5 K by the vibrating sample magnetometer (VSM) in PPMS.

3. Results and discussion

Prior to incorporating L5C5 VAN and LSMO layers into YBCO, single layers of L5C5 and LSMO were grown on STO substrates for magnetic property measurements. Fig. 1(a) and (b) show the M-H curves for the L5C5 and LSMO thin films, respectively, at different temperatures ranging from 20 K to 200 K. It is obvious that the hysteresis loops in both cases remain the same shape at different temperatures, which indicates their magnetic property remains at the superconductor working temperature range. In addition, it is clear that LSMO shows a higher magnetization and saturation remanence $\mathbf{M_{rs}}$ than L5C5 VAN, partly because of the non-magnetic CeO_2 in the L5C5 nanocomposites. By comparing $\mathbf{M_{rs}}$ of the two samples, $\mathbf{M_{rs}}$ (L5C5) ≈45 emu/cm^3 (here the magnetization of a single LSMO nanocolumn can be estimated to be 2.25×10^{-16} emu based on the volume of one single column as $5\times5\times20$ nm^3), which is lower than half of $\mathbf{M_{rs}}$ (LSMO) ≈ 200 emu/cm^3. One possible reason is that the incorporation of a second phase (CeO_2) into LSMO may cause the suppression of the double exchange interaction between the neighboring LSMO domains, which could deteriorate the magnetic property of LSMO [34]. Other factors to be considered include the film thickness variations and samples size for VSM measurements among samples. Moreover, interestingly, the L5C5 VAN exhibits higher coercive field $\mathbf{h_c}$ than the pure LSMO sample, because of the thin disordered regions at the LSMO|CeO_2 interface areas [34]. This disordered 2-phase boundary may lead to increased pinning effect [36], as well as larger lattice strain in the films [37]. Overall, both L5C5 VAN and pure LSMO thin films present strong magnetization response under applied magnetic field perpendicular to the sample surface.

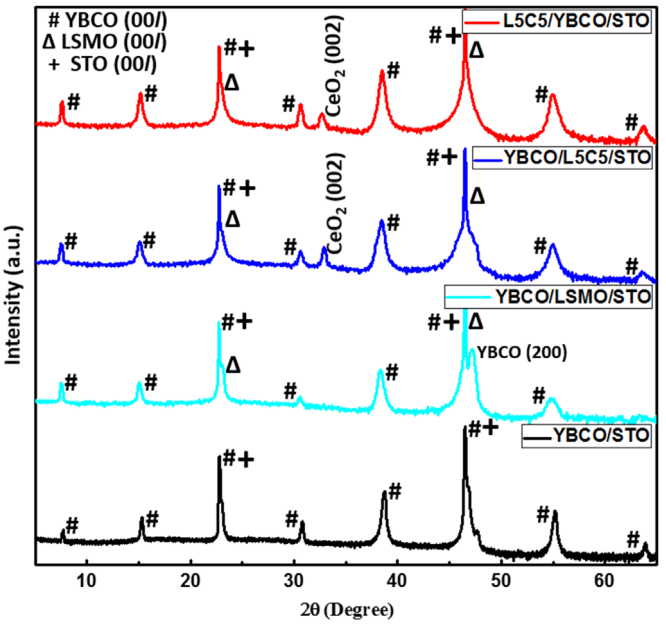

Fig. 2. θ−2θ XRD patterns of all the bilayer samples compared with the pure YBCO film.

L5C5 VAN was then incorporated into YBCO as either cap layer or buffer layer. As a comparison, a YBCO/LSMO bilayer stack was deposited to explore the pinning properties of a pure ferromagnetic LSMO layer. Fig. 2 shows the standard θ−2θ XRD scans of all the samples, symbols #, Δ and + represent YBCO (00*l*), LSMO (00*l*) and STO (00*l*) peaks, respectively. Apparently, for the L5C5/

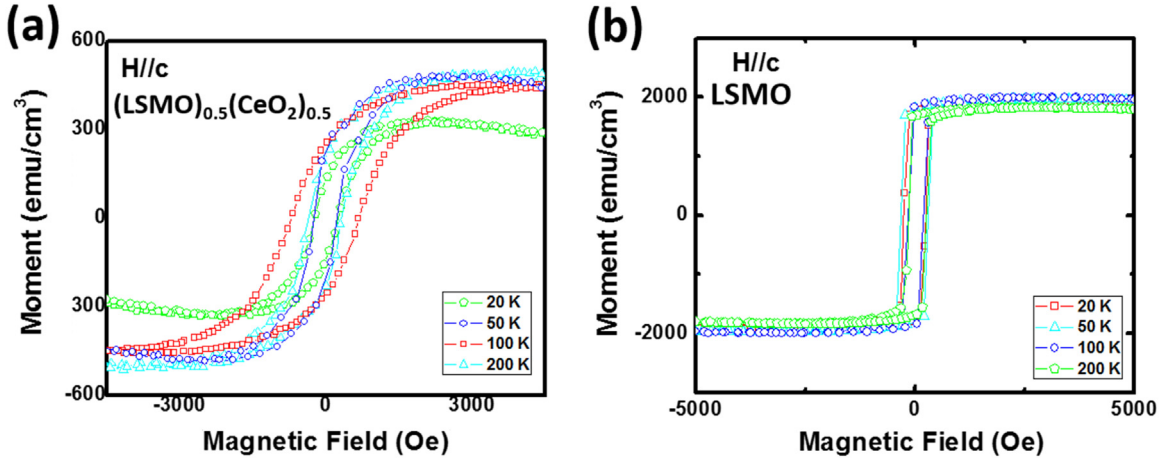

Fig. 1. *M–H* curves for (a) $(LSMO)_{0.5}$: $(CeO_2)_{0.5}$ VAN and (b) LSMO at 20 K, 50 K, 100 K and 200 K under magnetic field in the *c* direction.